A Revisit to Coastal Upwelling, With Reference to El Niño off South America

David Halpern
Jet Propulsion Laboratory
California Institute of Technology
Pasadena, CA 91109

****

Objective: Does w_{ek} enhance or weaken coastal upwelling?

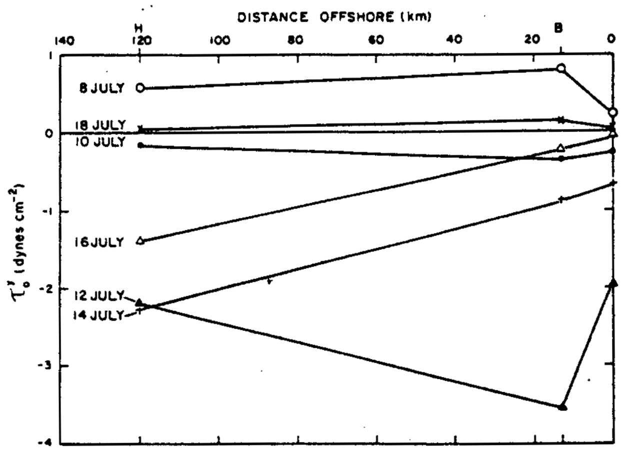

FIG. 3. Zonal gradient of low-pass filtered meridional components of wind stress occurring at 1200 GMT on alternate days during the interval 8–18 July in the region between the coastline and 120 km offshore. Wind stress at the coastline (Sand Lake) is assumed to be equal to the stress measured at Newport, Ore.

was approximately equal to the difference of the north-south wind-stress components; i.e.,

$$\mathrm{curl}_z\boldsymbol{\tau}_0 \sim \frac{\partial \tau_0^y}{\partial x} = \frac{\tau_0^y(\mathrm{B}) - \tau_0^y(\mathrm{H})}{L_{\mathrm{BH}}},$$

where $(\partial/\partial x, \partial/\partial y)$ are partial derivatives in the eastward (x) and northward (y) directions, $\tau_0^y(\mathrm{B})$ and $\tau_0^y(\mathrm{H})$ are the stresses at stations B and H, and L_{BH} the distance between the two stations. The wind-stress curl (Fig. 2) was computed from the difference of the low-pass north-south component time series. The summertime or seasonal mean value $(0.21\times10^{-7}$ dyn cm$^{-3})$ of the curl was positive and half as great as the standard deviation $(0.44\times10^{-7}$ dyn cm$^{-3})$. At the onshore station the strong southward wind stress associated with the 12 July storm occurred for a relatively short period of about 1.5 days, whereas at the offshore station high values were measured for a much longer period. For about 4 days prior to the occurrence of the maximum wind stress at the onshore station the curl was negative $[\tau_0^y(\mathrm{H}) > \tau_0^y(\mathrm{B})]$, reaching its maximum value of -1.3×10^{-7} dyn cm^{-3} on 12 July. The curl rapidly changed to positive values, reaching a maximum of about 1.3×10^{-7} dyn cm^{-3} on 14 July. Thus, within $\sim$50 h the wind-stress curl varied by 2.6×10^{-7} dyn cm^{-3}.

An order of magnitude calculation of the mean upward vertical velocity at the bottom of the Ekman layer [e.g., at about 20 m depth (Halpern, 1976; Smith *et al.*, 1971)] shows it to be about 10^{-4} cm s^{-1} offshore of Station B and 10^{-3} cm s^{-1} inshore of this site. On a shorter time scale, such as the period 12–16 July, the maximum offshore wind-stress curl $(1.3\times10^{-7}$ dyn cm$^{-3})$ may have produced an upward motion of magnitude 1×10^{-3} cm s^{-1} for a few days. However, the maximum nearshore wind curl $(10^{-6}$ dyn cm^{-3}; Fig. 3) could have been sufficient to account for the 10^{-2} cm s^{-1} vertical velocity inferred (Halpern, 1976) on 13 July from a time series of hydrographic data.

Halpern, 1976, JPO

Datasets

ERS-1/2 scatterometer
surface wind vector
$\Delta x = 25$ km, $\Delta y = 25$ km, $\Delta t = 3$ d
CERSAT dataset

TOPEX/Poseidon radar altimeter
sea surface height variations
$\Delta x = 7$ km, $\Delta y = 7$ km, $\Delta t = 10$ d
WOCE dataset

Time Interval

Glantz

Some years ago, scientists divided the tropical Pacific into four regions (Niño 1, Niño 2, Niño 3, Niño 4) to study sea surface temperature change. The difference between the monthly average sea surface temperature and the long-term mean monthly sea surface temperature, named sea surface temperature anomaly (SSTA), is a measure of the strength of El Niño or La Niña. Most recently, scientists have identified Niño 3.4 as a region that provides the most useful information on sea surface temperature changes related to the onset of El Niño. Australians have apparently shown more interest in SST changes in Niño 4, while Peruvians are most concerned about SST changes off their coast in regions called Niño 1 and Niño 2. In the diagram on this page (redrawn from the *Climate Diagnostics Bulletin* (see page 7)), the time series of Niño-3 SSTA clearly shows the El Niños of 1982–1983, 1986–1987, 1991–1994, and 1997–1998. The extended duration of the 1991–1994 El Niño remains unexplained. The combined Niño-1 and Niño-2 SSTA shows that the El Niños of 1982–1983, 1986–1987, and 1997–1998 had a double-peak structure

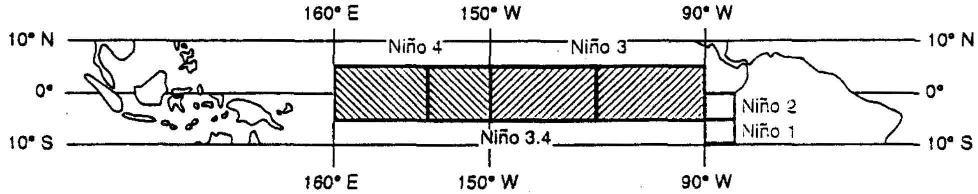

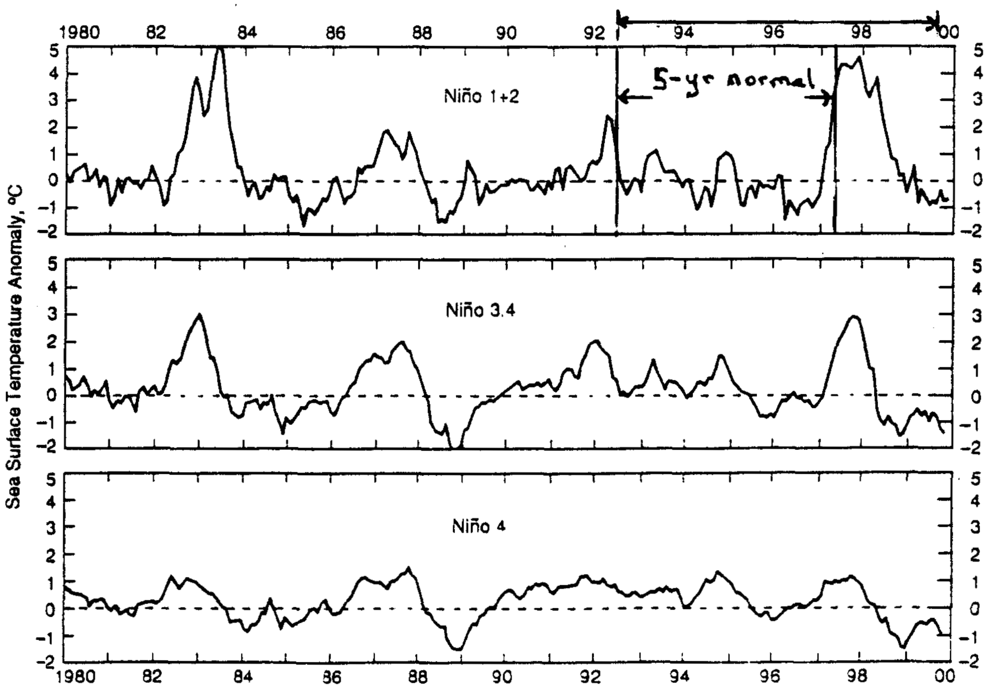

Glantz, 2000

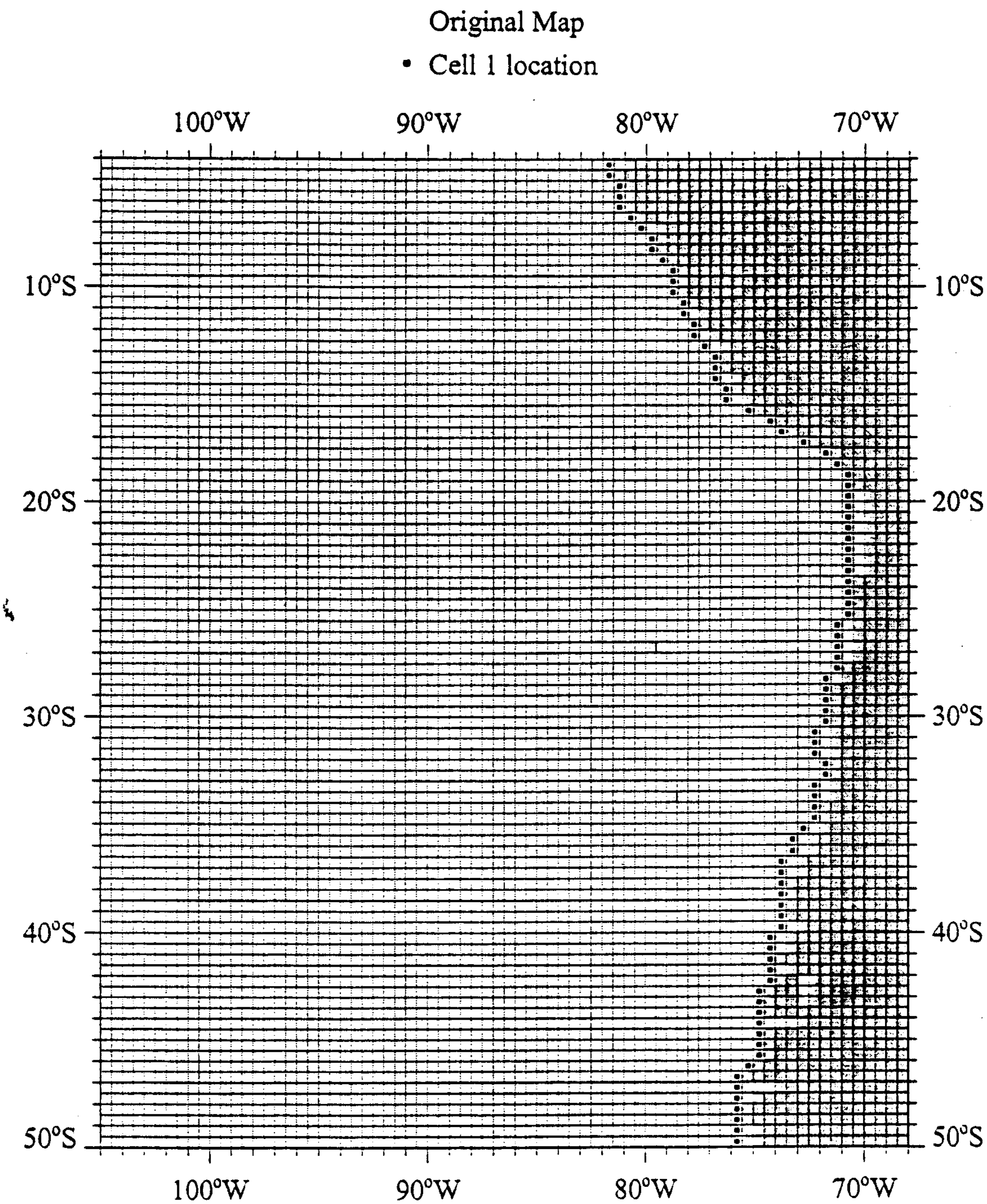
Original Map
• Cell 1 location
100°W
90°W
80°W
70°W
10°S
20°S
30°S
40°S
50°S

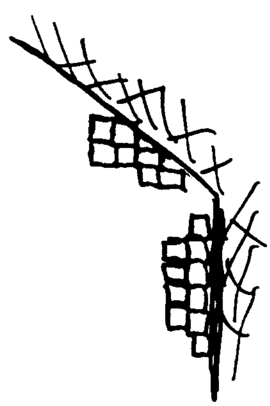

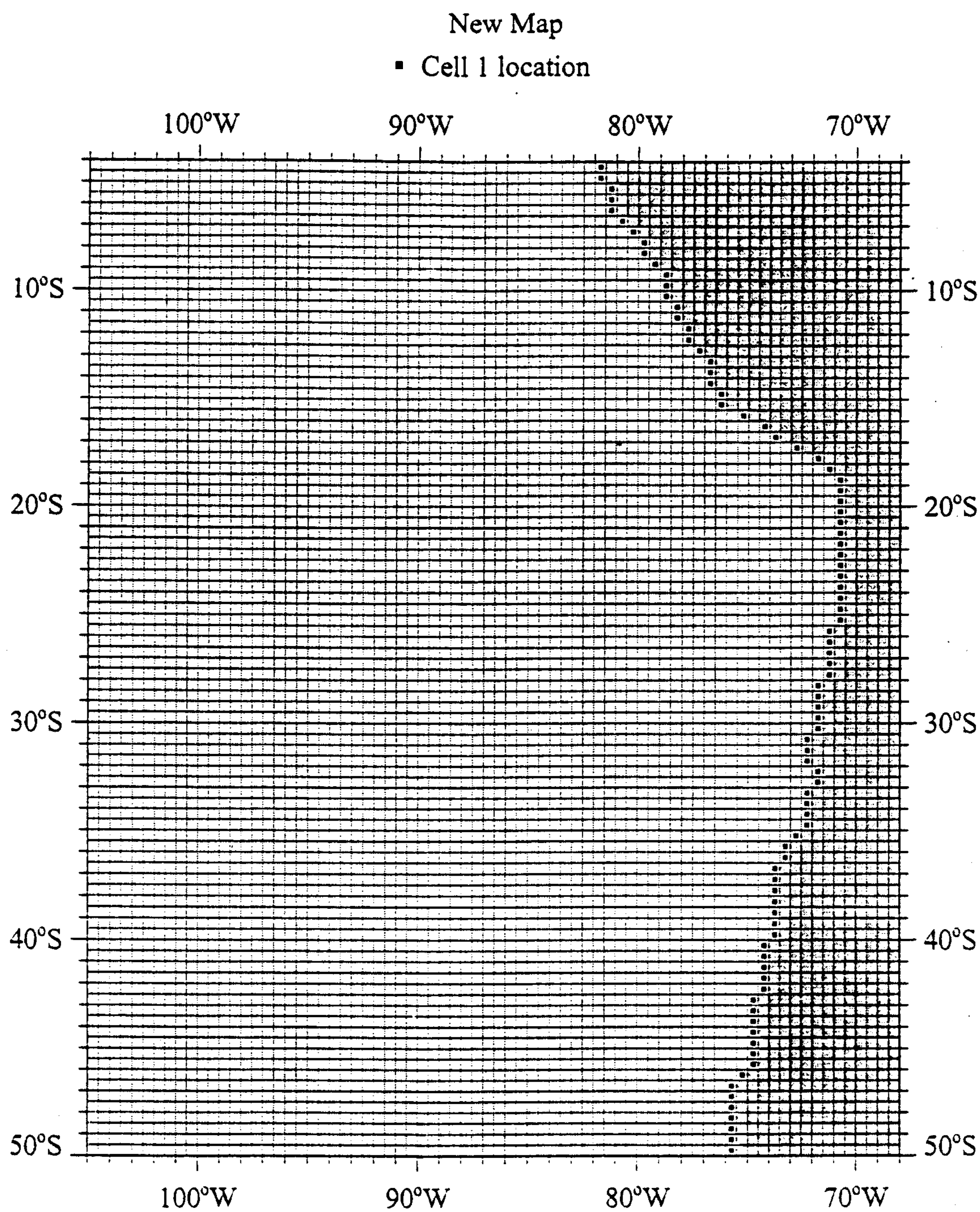
New Map
▪ Cell 1 location
100°W
90°W
80°W
70°W
10°S
20°S
30°S
40°S
50°S

Mean (5/1992-4/1997) Conditions

El Niño (1997-1998)

La Niña (1998-1999)

Conditions

ERS(IFR2) <Wek> 5/1992 - 4/1997, 10^{-6} m s^{-1}C

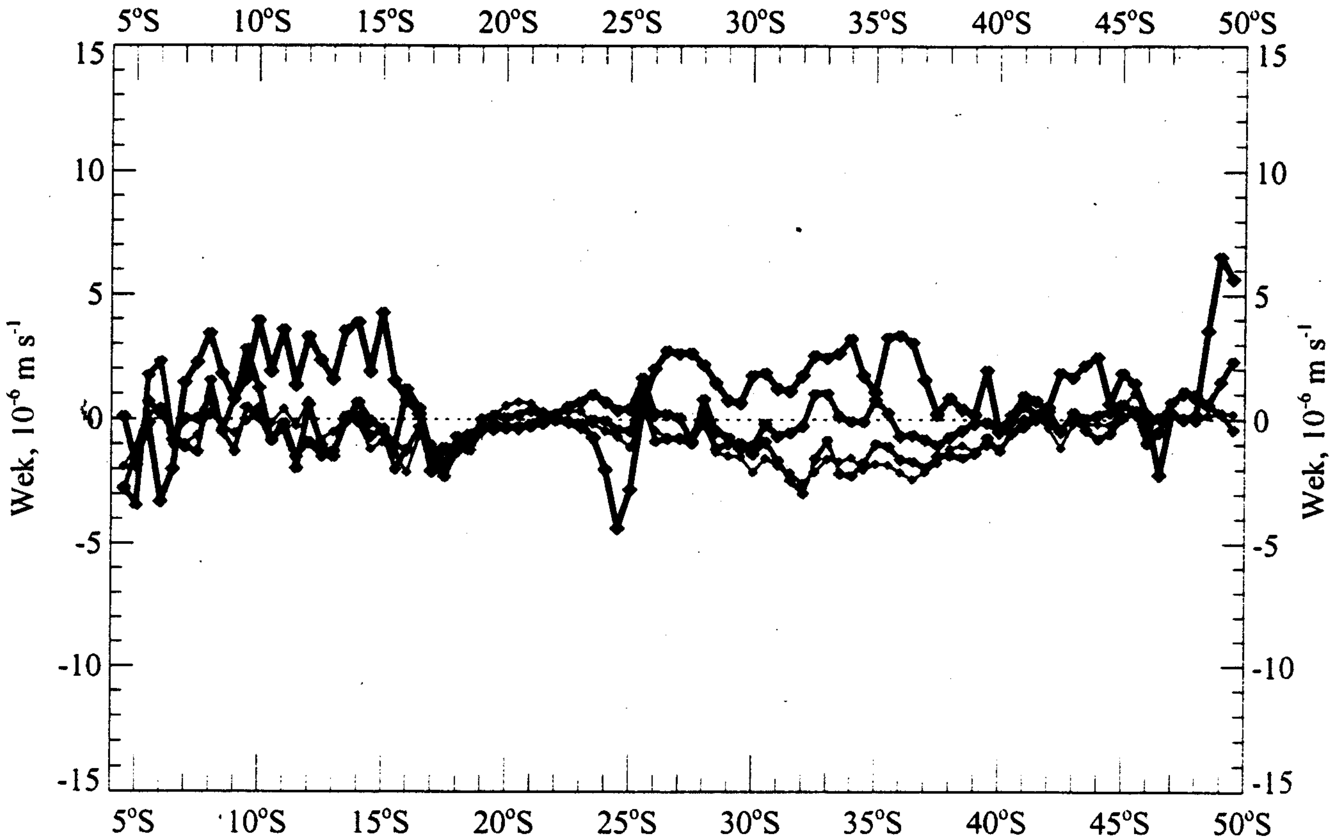

i = 1.5 Black (thick)

i = 3.5 Red (thick)

i = 5.5 Blue (thick)

i = 7.5 Black (thin)

Ekman suction enhances Ekman upwelling

Fri Mar 31 11:41:55 2000

ERS(IFR2) <CUI> 5/1992 - 4/1997, $m^2 s^{-1}$

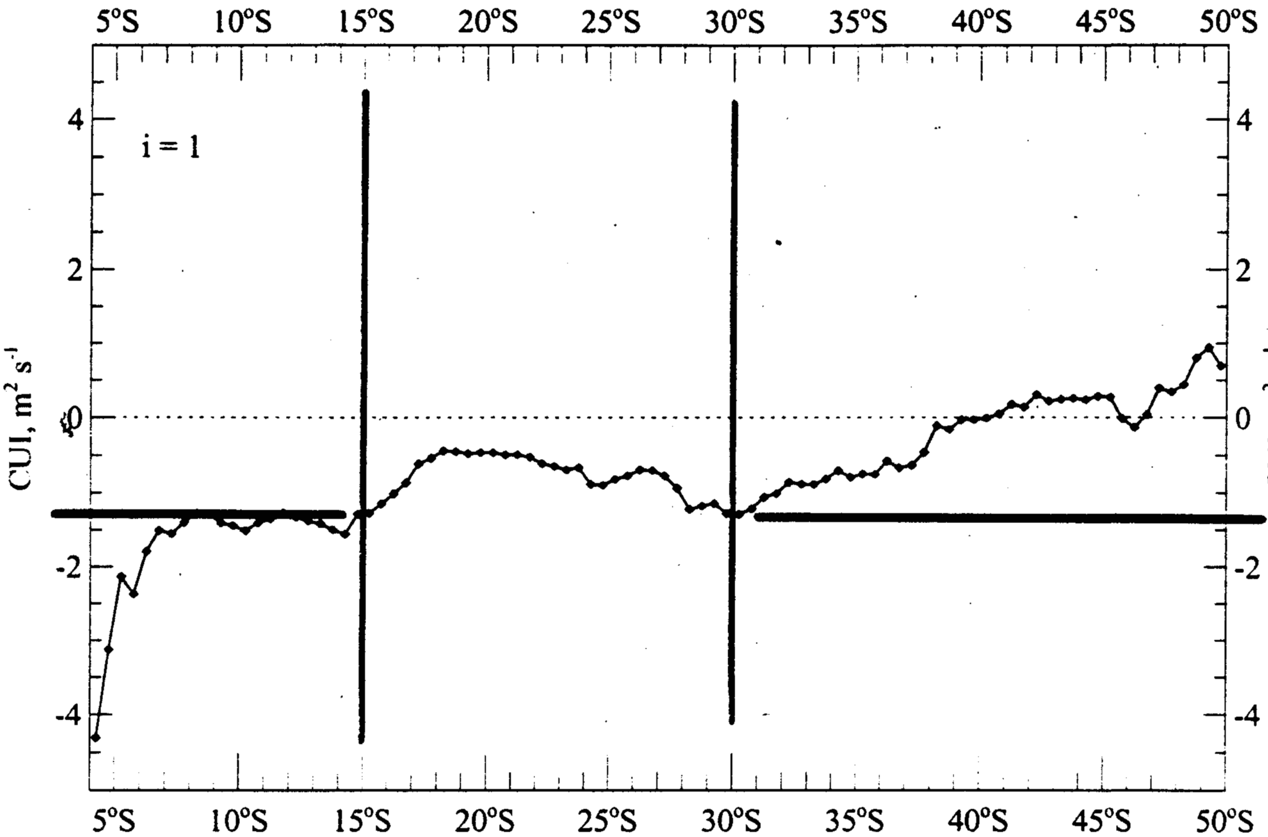

Fri Mar 31 14:03:37 2000

Mean (5/1992-4/1997) Conditions

$i = 1$

	15°S	30°S
CUI, $m^2\ s^{-1}$	-1.3	-1.4
w_{ek}, 10^{-6} m s^{-1}	3	2

Mean (5/1992-4/1997) Conditions

El Niño (1997-1998)

La Niña (1998-1999)

Conditions

Anomalies of SSH, 16.0°S - 17.0°S, i = 1

Anomalies of Wek, 14.25°S - 15.25°S, i = 1.5

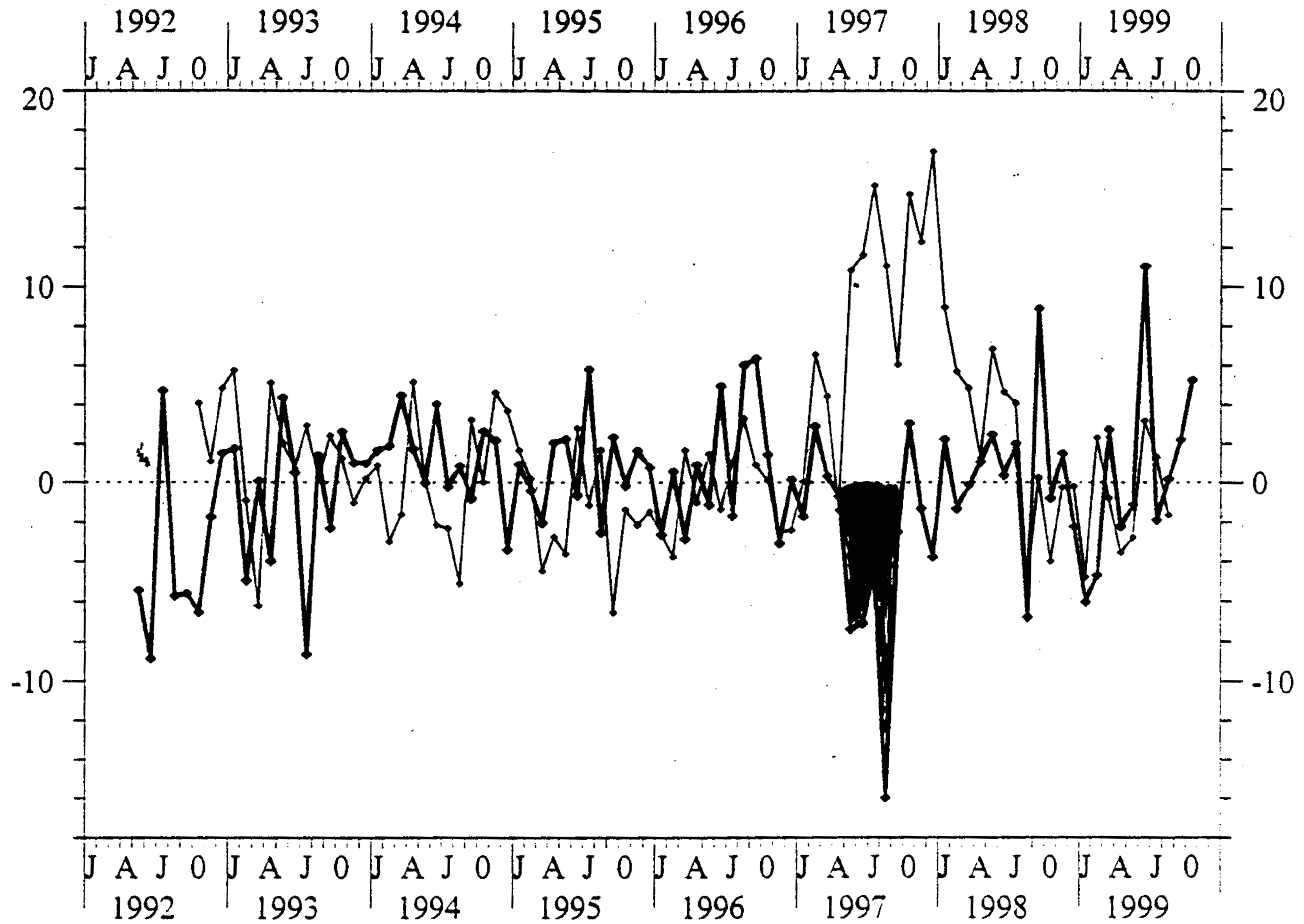

SSH Anomaly (THIN BLACK), cm

Wek Anomaly (THICK BLACK), 10^{-6} m s^{-1}

Anomalies 5-YR Mean & Standard Deviation [5/1992 - 4/1997]

	Mean	Std. Dev.	
Wek	-0.00	3.38	10^{-6} m s^{-1}

Anomalies 4-YR Mean & Standard Deviation [5/1993 - 4/1997]

	Mean	Std. Dev.	
SSH	-0.01	2.79	cm

Thu Mar 30 11:23:56 2000

SeaWiFS Chl-a for i = 1

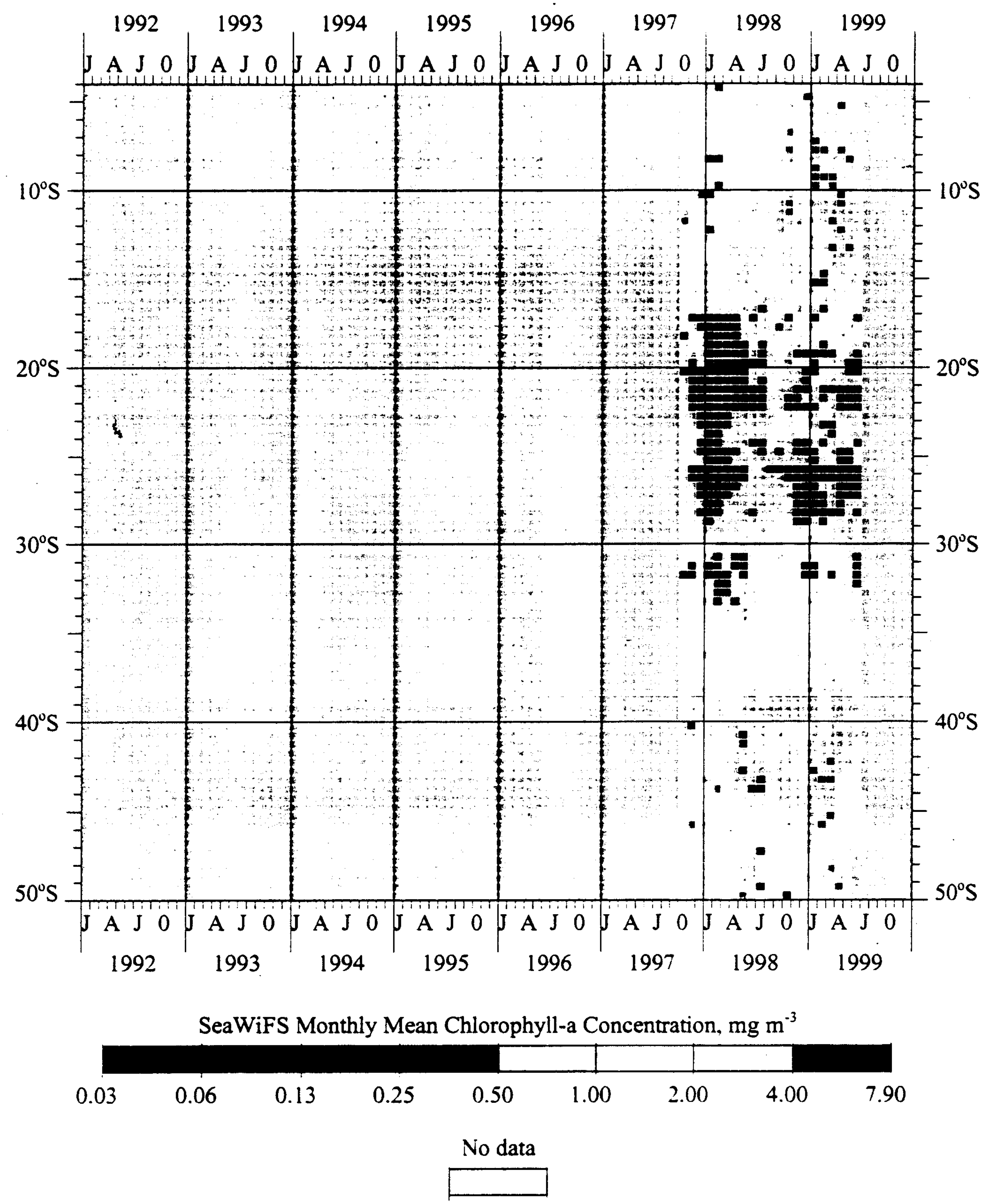

SeaWiFS Chl-a <10/1997 - 6/1999>, mg m^{-3}

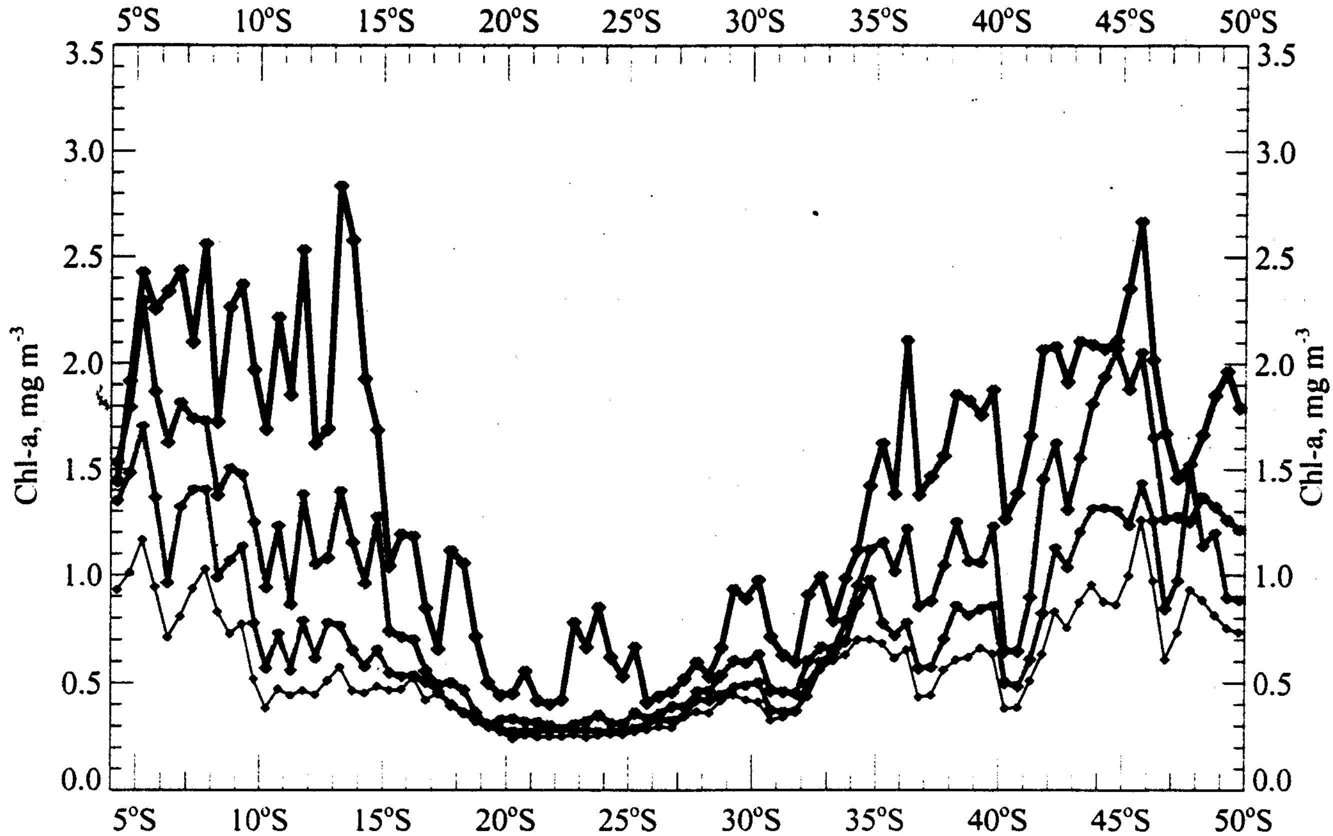

i = 1 Black (thick)

i = 2 Red (thick)

i = 3 Blue (thick)

i = 4 Black (thin)

Fri Apr 14 17:49:33 2000

SeaWiFS Chl-a <10/1997 - 6/1999>, mg m^{-3}

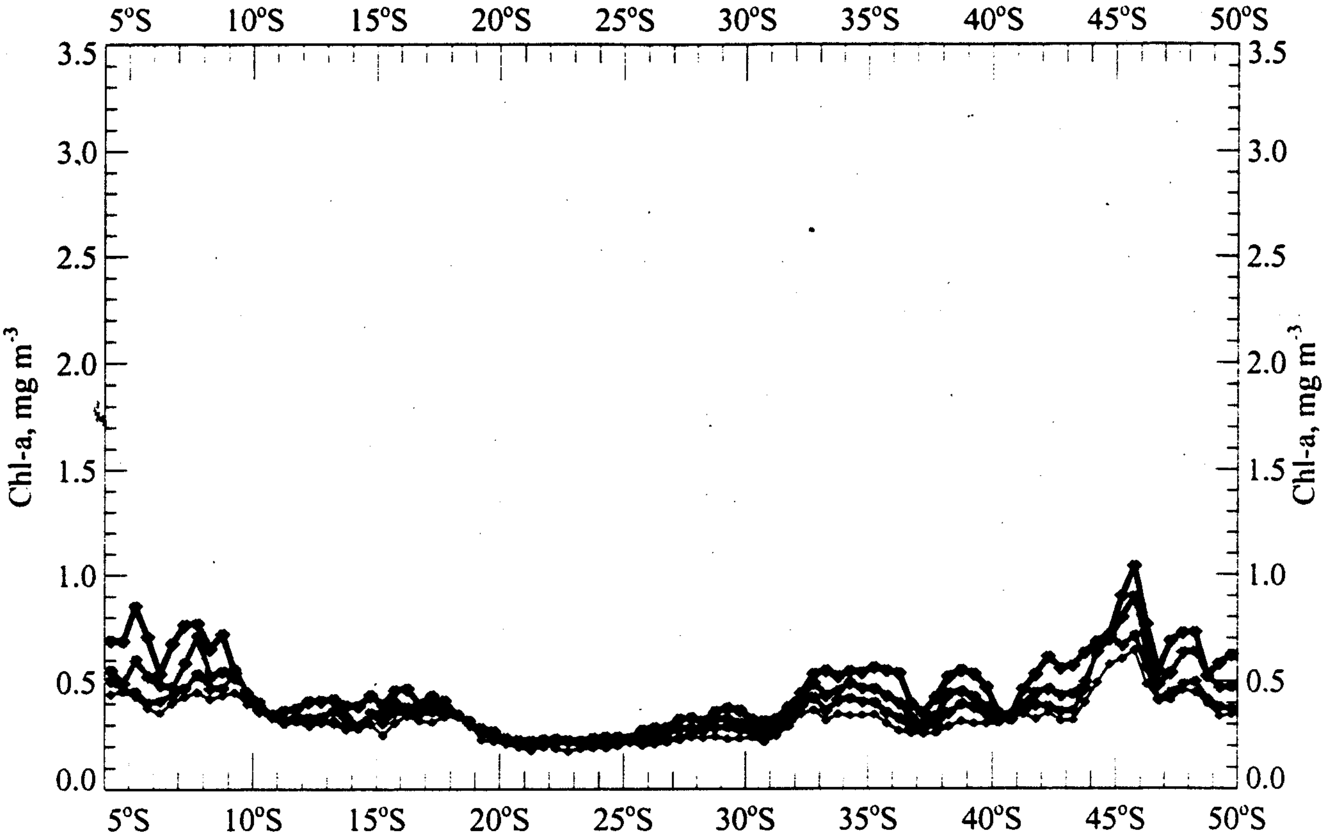

i = 5 Black (thick)

i = 6 Red (thick)

i = 7 Blue (thick)

i = 8 Black (thin)

Fri Apr 14 17:49:33 2000